Simulation of the Scale Factor of a Ductile Fracture of Polymer Blends and Composites on the Basis of the Specific Interphase Concept

V. G. Oshmyan, M. Yu. Shamaev, S. A. Timan

Institute of Chemical Physics, Russian Academy of Sciences, 4 Kosygin Street, 117977 Moscow, Russia

Received 20 February 2002; accepted 5 November 2002

ABSTRACT: The concept of interfacial layers surrounding inclusions in a host polymer is accepted as a basic source of the scale factor in the simulation of the large-strain deformation and fracture of polymer blends and composites. The essence of the phenomenon is the ductile–brittle transition if the polymer ligament thickness exceeds a critical value, which is determined by the nature of the polymer. Original texture-sensitive constitutive equations have been applied for the simulation of the polymer large-strain deformation. Two periodic structural models of composites have been used. The disperse component (elastomeric or rigid inclusion) has been replaced by a geometrically identical system of pores, which coincides with phenomena of elastomeric inclusion rupture in rubber-toughened plastics and debonding in particulate-filled composites. The local loss of stability of an elastic deformation is used as a composite fracture criterion. The specific properties of the interphase can be caused by a specific texture and by closeness to a free surface. This specificity is stated in the model by an improved plastic ability compared with that of a bulk polymer. Our simulations show that the percolation of an interfacial polymer provides the brittle–ductile transition. © 2003 Wiley Periodicals, Inc. J Appl Polym Sci 89: 2771–2777, 2003

Key words: composites; brittle; ductile; fracture; transitions

INTRODUCTION

Any kind of constitutive relations for continuum medium mechanics, which link strain (ε) and stress (σ) tensors, are invariant with respect to Cartesian coordinate (x) scale transformation: $x \rightarrow \lambda x$. This argument supports the conclusion that both macroscopic and microscopic mechanical behaviors of heterogeneous materials should not be dependent on the characteristic scale of the structure. In particular, it is natural to expect that a change in the particle size with the conservation of the volume fraction will not cause any noticeable mechanical response of a polymer blend or composite.

Nevertheless, it has undoubtedly been established that the inclusion diameter drastically affects the fracture parameters of polymer blends or composites. It has been found[1–3] that the brittle–ductile transition occurs not only with an increase in the rubber fraction but also with a decrease in the inclusion size in rubber-toughened plastics.

The ductile–brittle transition also holds for a particulate-filled polymer.[4–7] The quantitative parameters of the phenomenon, particularly the transition filler fraction (Φ_{tr}), are strongly influenced by the particle size. The scale dependencies of particulate-filled-polymer fracture parameters [e.g., the fracture toughness (F_t) and elongation to break (ε_b)] are more complicated than those of rubber-toughened plastics. That is, they are bell-shaped.[6] Therefore, an increase in the particle size (d) leads to a brittle–ductile transition at small d ($d < d_{max}$)[4,6] and to a ductile–brittle transition at large d ($d > d_{max}$).[5–7] It has been shown that the first transition is mostly caused by a drop in the debonding stress (σ_d), which provides, in turn, a decrease in the yield stress (σ_y). That is why an increasing branch of ε_b–d dependence is qualified as an adhesive factor of rupture. In the case of sufficiently large inclusions ($d > d_{max}$), debonding occurs mostly at the early stages of deformation. Therefore, the system becomes mechanically equivalent to porous media, as it is for rubber-modified polymers, especially in the case of cavitated inclusions. The decreasing character of the ε_b–d dependence is qualified[6] as a geometrical factor of rupture. This phenomenon of a general meaning is the subject of this simulation.

The deformation and fracture of porous media are simulated. Pores are supposed to be formed by either cavitation or debonding of the inclusion. The history of the pore formation is not a subject of this study. Therefore, the approach proposed is general in this sense and can be applied to a wide class of materials,

Correspondence to: V. G. Oshmyan (oshmyan@chph.ras.ru).

Contract grant sponsor: Russian Foundation for Basic Research; contract grant numbers: 00-03-33169, 01-03-32043, and 01-03-32237.

© 2003 Wiley Periodicals, Inc.

such as rubber-toughened plastics and particulate composites. In every case, pores in the model replace inclusions. The key idea of the simulation is the assumption concerning the formation of an interfacial layer of an increased plastic ability (cf. a bulk polymer). The thickness of a high-plastic layer is assumed to be dependent on the polymer nature, temperature, strain rate, and other conditions, but it is assumed to be independent of the particle content and size. Such invariance is the source of a simulated scale factor.

The special morphology of the interphase is not directly explained in this article. Readers are referred to publications[3,7–9] in which the interfacial layer concept is suggested and experimentally grounded for semicrystalline polymers such as high-density polyethylene[3,7] and polyamide 6.[8,9] It has been shown that in contrast to a spherulitic structure of a bulk polymer, the interphase is characterized by crystalline lamellae perpendicular to the inclusion boundary. The percolation of an interfacial polymer provides (accordingly to the authors' hypothesis) the brittle–ductile transition.

Recently, deformation of such a three-phase composite was simulated by Tzika et al.[10] The details of the texture were taken into account. Two different large-strain constitutive relations were used: a glassy polymer model[11,12] for the bulk matrix and a constrained hybrid model[13–16] for the crystalline interphase. The differences in the macroscopic diagrams, shear band nucleation, growth, and volumetric effects for the cases of thick, thin, and intermediate polymer ligaments were carefully elucidated and analyzed.

Nevertheless, the contribution of Tzika et al.[10] to the problem of the mechanisms of the scale effect on composite deformation and fracture still requires further development. First, no fracture criterion was introduced and applied to elucidate the ductile or brittle mode of the composite failure. Extended plastic flow seems to be a good indication of increased toughness. However, a direct simulation of composite failure is obviously desirable even if it is based on a simplified fracture criterion. Second, the critical ligament thickness criterion for the ductile–brittle transition is valid not only for semicrystalline polymers but also for glassy polymers,[2] which cannot be characterized by the special morphology of the interfacial layer. We believe that closeness to a free surface can be the reason for improved plasticity without serious morphological transformation. That is why it is sensible to also apply equations allowing the direct variation of the plastic ability. Third, the validity of a critical ligament thickness criterion should be confirmed independently of the constitutive model applied. Therefore, it is sensible to use various relations for the polymer finite deformation to simulate the phenomenon. Such a simulation is performed in this study on the basis of the original texture-sensitive constitutive model,[17,18] which is briefly defined later.

The problem discussed is very important for applications. Particulate-filled composites are widely used but unfortunately are mostly characterized by low fracture parameters. Simulations show certain ways of improving the toughness: a decrease in the inclusion size, the spatial arrangement of particles (to avoid aggregation), and filler and surface modification (to facilitate pore formation by debonding or cavitation).

The article is organized as follows. Constitutive equations for homogeneous polymers, structural assumptions for composites, accepted fracture criteria, and numerical algorithms are described in the next section. The micromechanical aspects of deformation, λ_{br} dependencies on the particle content and size, and regularities of the simulated ductile–brittle transitions are represented and discussed in the subsequent section. The main conclusions are summarized in the final section.

DEFINITIONS AND ASSUMPTIONS OF THE MODEL

Constitutive equations for polymer large-strain deformation

The recently proposed[17,18] texture-sensitive constitutive model for homogeneous polymer large deformation and ductile fracture is used for the targets of our simulations. The basic points of the model are listed next.

The polymer texture is characterized by a distribution in the polymer fragment orientation:

$$f(\mathbf{p})d\mathbf{p} \tag{1}$$

This determines a portion of the polymer fragments at a given point (x) of the space oriented in the infinitesimal area ($d\mathbf{p}$) of a unit sphere around a given direction ($\mathbf{p}$). The term *polymer fragment* is supplied by a flexible physical sense dependent on a polymer and on the conditions and stage of deformation. In particular, the term can refer to a polymer crystal or to a segment of a polymer chain. Moreover, several kinds of polymer fragments of different physical meanings can be introduced. A bifragmental model was applied[18] for the simulation of the large-strain deformation of a semicrystalline polymer.

The kinematics are described in the framework of the multiplicative law for deformation gradients:

$$\mathbf{F} = \frac{\partial x}{\partial X} = \mathbf{F}_e \circ \mathbf{F}_p \tag{2}$$

where $\mathbf{F}_e$ and $\mathbf{F}_p$ are elastic (reversible) and plastic (irreversible) multipliers, respectively. Equation (2) in-

dicates the local representation of the mapping of the reference coordinates (X) to the current coordinates (x) as a complex mapping with an intermediate irreversible state (X_p):

$$x = x(X) = x[X_p(X)], \quad \mathbf{F}_p = \frac{\partial X_p}{\partial X}, \quad \mathbf{F}_e = \frac{\partial x}{\partial X_p} \tag{3}$$

The symmetric representation of the elastic deformation gradient [$(\mathbf{F}_e)^T = \mathbf{F}_e$] and the logarithmic definition of the elastic strain tensor

$$\varepsilon = \log \mathbf{F}_e \tag{4}$$

are used.

Elastic constitutive equations for the polymer of the structure described by the orientational distribution [$f(\mathbf{p})$] are determined in terms of the elastic potential (U_e)

$$U_e = \tfrac{1}{2} C^{(f)}_{ijkl} \varepsilon_{ij} \varepsilon_{kl} \tag{5}$$

in current spatial variables (x).

The elasticity tensor ($C^{(0)}_{ijkl}$) for perfectly oriented fragments is supposed to be anisotropic. In particular, the crystal modulus in the chain direction can be several orders of magnitude greater than that in the transverse direction. The tensor $C^{(f)}_{ijkl}$ is defined in the model by the rule of mixture:

$$C^{(f)}_{ijkl} = \langle C_{ijkl}(\mathbf{p}) \rangle_{f(p)} = \int C_{ijkl}(\mathbf{p}) f(\mathbf{p}) d\mathbf{p} \tag{6}$$

This corresponds to the assumption of strain uniformity with respect to fragments that are differently oriented but similarly posed in the space.

The kinetics of plastic flow, that is, the transformation rate of the plastic deformation gradient ($\mathbf{F}_p$), is multiplicatively defined in the model:

$$\mathbf{F}_p(t) = \mathbf{F}^a_p(\Delta t) \mathbf{F}_p(t - \Delta t) \tag{7}$$

The explicit definition of an additional plastic deformation gradient [$\mathbf{F}^a_p(\Delta t)$] is given in refs. 17 and 18. In fact, it can be represented as a functional dependence (Λ_p) of the plastic strain rate ($\dot{\varepsilon}_p$) on the shear stress (τ) and orientational distribution (f):

$$\dot{\varepsilon}_p = k_p \Lambda_p(\tau, f) \tag{8}$$

Equation (8) corresponds to a slip mechanism of plastic flow in the polymer fragment orientation. Therefore, the polymer fragments oriented in the direction of the elastic tension contribute nothing to $\dot{\varepsilon}_p$. On the contrary, polymer fragments contribute the maximum to $\dot{\varepsilon}_p$ if their slope to the tension direction is 45°. The general plastic ability of a polymer is governed by a model parameter (k_p).

The evolution of the structure, that is, the kinetics of transformation of the orientational distribution, is closely coupled to irreversible deformations. We also refer to refs. 17 and 18 for explicit definition. Similarly to eq. (8), the operator Λ_o, determines the orientational rate ($\dot{f}$) for a given stress σ and value of f:

$$\dot{f} = k_o \Lambda_o(\sigma, f) \tag{9}$$

Equation (9) follows the elastic transformation rule for every given orientation $\mathbf{p}$. For instance, uniaxial drawing provides the preferable orientation of the fragments in the drawing direction, and fragments oriented in the tension direction do not exhibit reorientation. The orientational rate in eq. (9) is governed by a model parameter (k_o).

The fracture criterion is determined as a condition of the local instability of the elastic part of deformation. It is worthwhile to note that the large-strain uniform deformation of solids is mostly unstable. The formation of a shear band, craze, and neck is typical of strain localization. However, such instabilities are not considered sources of fracture if they are caused by localization of the plastic flow, whenever elastic deformation remains stable. The stability loss of elastic deformation causes a divergence in the numerical scheme. This coupling is explored as an indicator of fracture in simulations.

Of course, the criterion used is local. It simulates only nucleation, not the propagation of the defect. Therefore, its application is not completely sufficient for the global analysis of the material's failure. This insufficiency is a general problem of fracture mechanics. Nevertheless, local criteria are widely accepted and successfully used in numerous studies,[19–21] especially if a comparable analysis of the ultimate characteristics is a target of simulation, which is the case of this work. In particular, a corresponding approach was recently applied by us to a comparison of F_t of particulate-filled composites with high and low adhesive strengths.[18,22]

In fact, the criterion of the loss of stability of elastic deformation can be reformulated as a widely used stress criterion of fracture. However, the critical stress–strain state (SSS) strongly depends on the material's texture. It seems to be natural to define this dependence with stability loss conditions, as done in this study.

Structural model

The assumptions concerning the composite structure are similar to those accepted in ref. 18 for binary

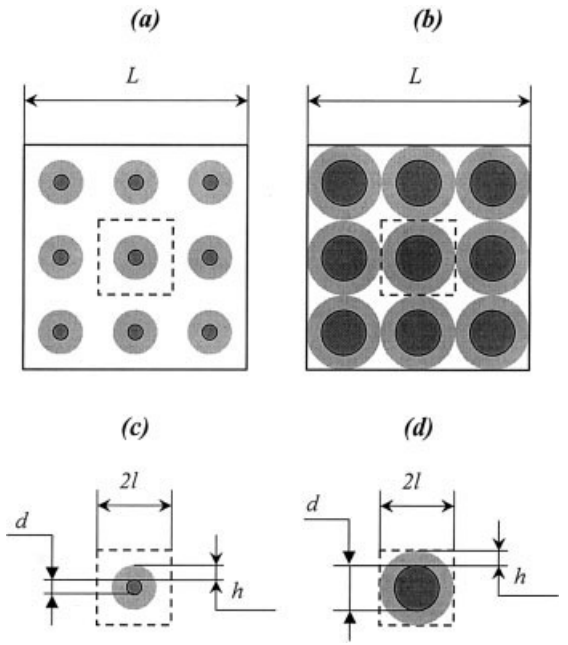

Figure 1 Periodic two-dimensional structural models for (a,b) the composite and (c,d) the corresponding periodicity cells. The inclusions, bulk polymer, and high-plastic interfacial layers are depicted by black, white, and gray, respectively. (a,c) Nonpercolated and (b,d) percolated high-plastic regions are shown.

composites (the composite sphere model of Hashin[23] was used in an alternative simulation;[19] it is important to note that the results obtained are very close to those of ref. 18). Two-dimensional boundary value problems are considered. Inclusions of identical shape and size (dark regions in Fig. 1) are supposed to be periodically distributed in the polymer matrix (white and light regions in Fig. 1).

Every inclusion is surrounded by a high-plastic polymer layer (light regions in Fig. 1) of a fixed thickness (h), which is assumed to be a material parameter independent of the particle fraction (Φ) and size (d). The percolation of high-plastic regions occurs if a certain relation between h, Φ, and d holds true. Obviously, the relation depends on the shape and disposition of the inclusions. In particular, in the case of the square disposition of a circular inclusion (Fig. 1), the percolation threshold is defined as follows:

$$d^2 = \alpha\Phi(d + 2h)^2 \tag{10}$$

where α is equal to $4/\pi$. The circular shape of the inclusions is less convenient than the square one for further numerical simulations. That is why the square shape of the inclusions has been chosen. Square [Fig. 2(a,c)] and chesslike [Fig. 2(b,d)] dispositions of their centers have been considered. Percolation thresholds for square and chesslike structural models are also defined by eq. (10) with $\alpha = 1$ and $\alpha = 2$, respectively.

Boundary value problem and numerical scheme for its solution

Mathematical techniques for the statement and solution of the boundary value problem, which describes the large-strain deformation of either binary or multiphase composites of periodic and composite sphere structures, are defined in refs. 18 and 22, respectively. Therefore, it is sensible not to overload readers with cumbersome details, so we only briefly list the main points of the approach related to a periodic structural model.

Homogenization theory (see refs. 24 and 25) reduces a macromechanical description of a periodically homogeneous medium [Fig. 1(a,b)] to the solution of the boundary value problem for a representative periodicity cell [Fig. 1(c,d)]. Mirror symmetry, both of the structure and macroscopic load, which are supposed to be true, provides the possibility of an additional diminution of the integration domain to the quarter of a periodicity cell (Fig. 2) and of a replacement of periodic boundary conditions by conventional ones:

$$x_i|_{X_i=0} = 0, \quad x_i|_{X_i=L} = \hat{\lambda}_i(t)L, \quad \left.\frac{\partial x_j}{\partial X_i}\right|_{X_i=0} = 0, \quad j \neq i \tag{11}$$

with given axial values $\hat{\lambda}_i(t)$ of a macroscopic deformation gradient $\hat{\mathbf{F}}_{ij}(t) = \hat{\lambda}_i(t)\delta_{ij}$.

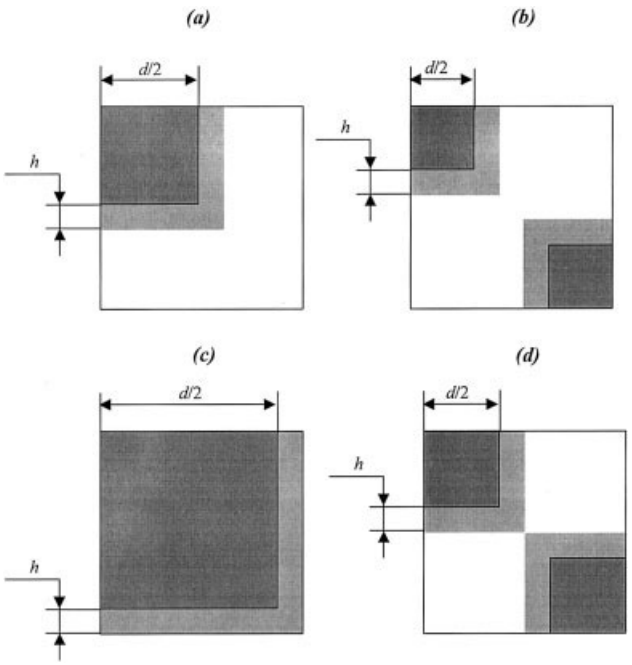

Figure 2 Quarters of periodicity cells corresponded to (a,c) quadric and (b,d) chesslike structural models. The indications of the components and the percolation of the high-plastic regions are the same as those given in Figure 1.

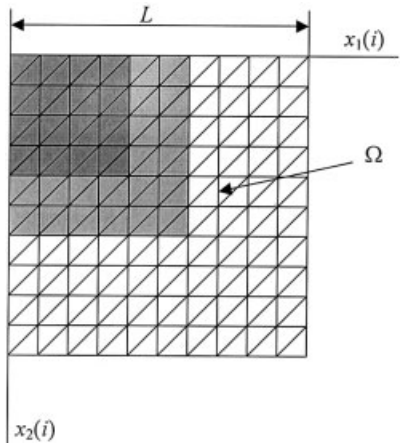

Figure 3 Sketch of the FE system for the quarter of the periodicity cell.

An original version of the finite element (FE) method[18,22] is applied to the numerical solution of the boundary value problem [eq. (11)]. The system of triangular FEs is depicted in Figure 3. The deformation of every triangle is interpolated by a uniform SSS based on the node positions (x_i). Therefore, the current configuration of the nodes is sufficient for an approximate definition of the SSS in a composite.

The solution of the elastic problem is the most cumbersome part of the algorithm. The FE interpolation of the mapping $x(X)$ leads to the approximation of the total elastic energy ($\tilde{U}_e$) of the node position:

$$\hat{U}_e = \int\int_{\omega(t)} U_e(t, x)dx = \int\int_{\Omega} U_e[t, x(X)] \frac{\partial x}{\partial X} dX \cong \tilde{U}_e = \sum_k U_e^{(k)} s^{(k)} \quad (12)$$

The energy density [eq. (5)] is determined by the kinematical decomposition [eq. (2)] and the strain and elasticity tensors [eqs. (4) and (6)]. Ω and $\omega(t)$ are used for the initial and current configurations of the quarter of the periodicity cell (Fig. 3). $U_e^{(k)}$ and $s^{(k)}$ are the elastic energy and area of the kth FE, respectively.

The minimization of $\tilde{U}_e$ [eq. (12)] by a proper choice of the node position [$x_i(t)$], with boundary conditions [eq. (11)] taken into account, is a way of solving the elastic problem. The iteration procedure, $(s) \rightarrow (s + 1)$, has been elaborated for this purpose. It is based on a second power approximation of the function $\tilde{U}_e$:

$$\tilde{U}_e \approx \tilde{\tilde{U}}_e = \tilde{U}_e[x^{(s)}] + \sum_i \frac{\partial \tilde{U}_e}{\partial x_i}[x^{(s)}][x_i^{(s+1)} - x_i^{(s)}] + \sum_{i,j} \frac{\partial^2 \tilde{U}_e}{\partial x_i \partial x_j}[x^{(s)}][x_i^{(s+1)} - x_i^{(s)}][x_j^{(s+1)} - x_j^{(s)}] \quad (13)$$

This reduces the minimization problem at every iteration step, $(s) \rightarrow (s + 1)$, to the linear system of algebraic equations:

$$\frac{\partial \tilde{\tilde{U}}_e}{\partial x_i^{(s+1)}} = 0 \quad (14)$$

Then, plastic deformation gradients [$\mathbf{F}_p^{(k)}t$] and orientational distributions [$f^{(k)}(t)$] for each of the kth FEs are calculated with the kinetics of plastic flow and the laws of the structural evolution (see the previous subsections).

RESULTS AND DISCUSSION

Parameters of the model and loading conditions

The macroscopic loading conditions of uniaxial drawing with a fixed drawing rate ($\dot{\varepsilon} = 0.1$) have been stated in every computer experiment.

The elastic properties of both bulk and interfacial polymers with perfectly oriented fragments are characterized by the following values in dimensionless units: $E_a = 2.5$ (axial Young's modulus in the direction of orientation), $E_t = 0.025$ (Young's modulus in the transverse direction), $\nu_{ta} = 0.2$ (Poisson ratio of transverse compression caused by axial tension), and $\mu = 0.02$ (shear modulus).

The value of k_o, which is responsible for the rate of structural evolution, also does not differ for the two polymers in the simulations and is equal to 0.5. The parameter k_p, which governs by the plastic ability, has been verified from 1.5 for bulk polymers to 2.5 for interfacial polymers. Such a difference results in a diminution of σ_y from 0.55 to 0.35 and in an increase of λ_{br} from 1.76 to 6.2 (Fig. 4).

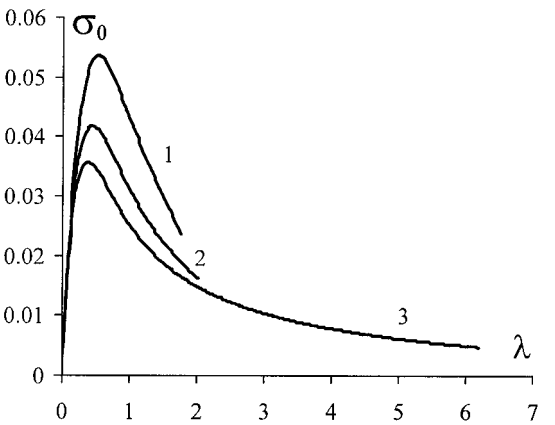

Figure 4 Drawing diagrams for a composite of a quadric structure calculated (1) for a low-plastic matrix, (3) for a high-plastic matrix, and (2) for a ratio of 0.2 of the thickness of the high-plastic interfacial layer to the linear size of Ω of the periodicity cell (Fig. 3). The diagrams correspond to $\Phi = 25\%$.

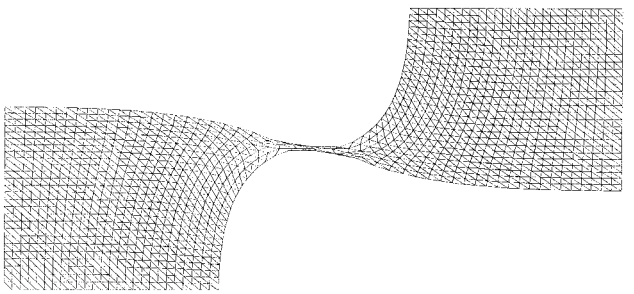

Figure 5 Large-strain deformation of the mesh corresponding to a porous high-plastic polymer with a chesslike structure. The filler fraction, $\Phi = 21.16\%$, is close to 25%, the maximum for a given structural model.

Deformation features

The model predicts an essential difference in the composite plastic ability caused by a variation of the relative thickness of a high-plastic layer (Fig. 4). In particular, σ_y decreases from 0.55 to 0.35. The λ value rises from 1.76 to 6.2 (the fracture criterion in the simulations consists of a loss of elastic stability).

Therefore, the high-plastic ability of the polymer matrix, particularly in the presence of a well-developed cluster formed of a high-plastic polymer, provides the same for a composite if cavitation on inclusions occurs during the early stages of deformation. The large-strain deformation of the mesh in a porous high-plastic polymer of a chesslike structure is shown in Figure 5. The value of the analyzed filler fraction, $\Phi = 21.16\%$, is close to 25%, which is near the maximum packing for the structural model. Therefore, the distance between neighboring inclusions (pores) is very small. Nevertheless, the possibility of large-strain deformation is still possible. The second interesting feature is seen in the deformation image in Figure 5. The corner points of the boundary (vertices of square inclusions) do not drastically restrict the composite plastic ability and undergo a considerable smoothening in the process of large-strain deformation.

Fracture features

The λ_{br} values of composites under the assumption of interfacial high-plastic layer formation are examined and discussed in this section. Two structural models, quadric and chesslike, are analyzed. Both suggest the periodic disposition of identical square inclusions. Their centers are supposed to be suited to the sites of a square lattice [Fig. 2(a,c)] for the first and a chesslike order for the second.

λ_{br} versus the ratio of the inclusion (pore) size to the thickness of the interfacial layer of a high-plastic polymer at various values of Φ are shown in Figure 6. The model predicts ductile–brittle transitions for both of the chosen structural models. This transition is sharper for the quadric structural model.

The laws of the transition qualitatively coincide with that experimentally observed for rubber-toughened plastics[1–3] and particulate-filled composites.[4–9] In particular, an increase in the inclusion (pore) fraction shifts the transitional inclusion size to lower values. However, the modeling of a large-strain deformation in frameworks of different structural assumptions shows that one should be careful in the direct application of a critical ligament thickness criterion for the description of the transitional point. The relative size values, which correspond to a percolation of a high-plastic polymer [eq. (10)], are depicted in Figure 6 by dotted vertical lines. The transitional size is very well described by the percolation condition [Fig. 6(a)]. However, the corresponding values are essentially lower than the values calculated with eq. (8) for a chesslike structural model. The difference is primarily caused by a remarkable nonuniformity of percolated interfacial layers in their thickness in the case of a chesslike structure [light regions in Fig. 2(d)]. On the contrary, the interfacial layers are perfectly uniform in thickness for a quadric structure [Fig. 2(c)]. Therefore, a more perfect cluster of the high-plastic region is necessary for high-plastic properties of a composite than what is formed just below a percolation point in the case of a chesslike structure. The assumptions of the quadric model provide a perfect connection between the interfacial layers at the moment of percolation.

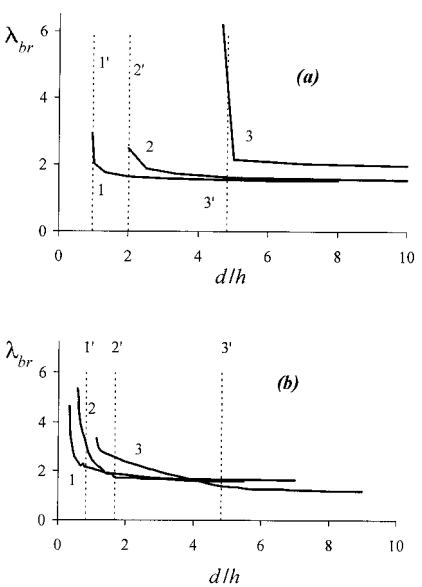

Figure 6 Ultimate elongation (λ_{br}) versus the relative inclusion size (ratio of the inclusion size to the thickness of the interfacial layer, or d/h), calculated at (a) Φ = (1) 10, (2) 25, and (3) 50% for composites of a quadric structure and (b) Φ = (1) 4, (2) 10, and (3) 25% for composites of a chesslike structure. The percolation thresholds for corresponding structures [eq. (8)] are depicted by dotted lines.

CONCLUSIONS

1. A novel model of the large-strain deformation and fracture of polymer blends and composites has been elaborated on the basis of the original texture-sensitive constitutive relations for monophase polymer solids.
2. It is suggested in simulations that the cavitation of inclusions occurs during the early stages of deformation. Therefore, the modeling of the large-strain deformation is performed under the replacement of the inclusions by pores of identical shape and size.
3. The special properties of the interfacial polymer layer, particularly its increased plastic ability, are assumed. It is thought that the thickness of the interfacial layer is determined by the polymer nature and the conditions of the composite preparation and testing, but it is independent of the inclusion content and size.
4. Two structural models have been used for the comparative analysis. The quadric position of square inclusions is first. It provides perfect uniformity of interfacial layers in thickness just after their percolation. The second model suggests chesslike positions of square inclusions, and a poor connection of interfacial layers occurs at the percolation point.
5. The interfacial layer concept greatly assists in the quantitative study of deformation and fracture. The deformation diagrams and micromechanical aspects of deformation have been analyzed. The transition from ductility to brittle fracture has been simulated and discussed. The results qualitatively coincide with the experimentally observed laws for two types of polymer systems: rubber-toughened polymers and particulate-filled composites (law of adhesion). The validity of the critical ligament system criterion has been discussed.

References

1. Wu, S. Polymer 1985, 26, 1855.
2. Wu, S. J Appl Polym Sci 1988, 35, 549.
3. Bartczak, Z.; Argon, A. S.; Cohen, R. E.; Weinberg, M. Polymer 1999, 40, 2331.
4. Pukanszky, B.; Fekete, E.; Tudos, F. Makromol Chem Macromol Symp 1989, 28, 165.
5. Fu, Q.; Wang, G.; Shen, J. J Appl Polym Sci 1993, 49, 673.
6. Dubnikova, I. L.; Gorenberg, A. Y.; Oshmyan, V. G. J Mater Sci 1997, 32, 1613.
7. Bartczak, Z.; Argon, A. S.; Cohen, R. E.; Weinberg, M. Polymer 1999, 40, 2347.
8. Muratoglu, O. K.; Argon, A. S.; Cohen, R. E. Polymer 1995, 36, 921.
9. Muratoglu, O. K.; Argon, A. S.; Cohen, R. E. Polymer 1995, 36, 2143.
10. Tzika, P. A.; Boyce, M. C.; Parks, D. M. J Mech Phys Solids 2000, 48, 1893.
11. Boyce, M. C.; Parks, D. M.; Argon, A. S. Mech Mater 1988, 7, 15.
12. Arruda, E. M.; Boyce, M. C. Int J Plast 1993, 9, 697.
13. Parks, D. M.; Ahzi, S. J Mech Phys Solids 1990, 38, 701.
14. Lin, L.; Argon, A. S. Macromolecules 1992, 25, 4011.
15. Lee, B. J.; Argon, A. S.; Parks, D. M.; Ahzi, S.; Bartczak, Z. Polymer 1993, 34, 3555.
16. Lee, B. J.; Ahzi, S.; Asaro, R. J. Mech Mater 1995, 20, 1.
17. Oshmyan, V. G. Polym Sci B 1995, 37, 17.
18. Herrmann, K. P.; Oshmyan, V. G.; Shamaev, M. Y.; Timan, S. A. Polym Sci C 2002, 44, 9.
19. Rabotnov, Y. N. Mekanika Deformiruemogo Tverdogo Tela (in Russian); Nauka: Moscow, 1988.
20. Kachanov, L. M. Osnovy Mekaniki Razrusheniya (in Russian); Nauka: Moscow, 1974.
21. Narisava, I. Prochnost Polimernykh Materialov (in Russian); Khimiya: Moscow, 1987.
22. Muravin, D. K.; Oshmyan V. G. J Macromol Sci Phys 1999, 38, 749.
23. Hashin, Z. AIAA J 1966, 4, 1411.
24. Bakhvalov, N. S.; Panasenko, G. P. Averaging Processes in Periodic Media: Mathematical Problems in Mechanics of Composite Materials; Kluwer Academic: Dordrecht, 1989.
25. Bensoussan, A.; Lions, J.-L.; Papanicolaou, G. Asymptotic Methods in Periodic Structures; North Holland: Amsterdam, 1978.